DISTORTION ANALYSIS IN LASER WELDING OF ULTRA HIGH STRENGTH STEEL

Karl Fahlström[1,2], Oscar Andersson[3,4], Urban Todal[3], Arne Melander[1,4], Lars-Erik Svensson[2], Leif Karlsson[2]

Swerea KIMAB[1], University West, Engineering Science[2], Volvo Cars Corporation[3], XPRES, KTH Royal Institute of Technology[4]

karl.fahlstrom@swerea.se

Abstract: Due to increased demands on reduced weight in automotive industries, the use of ultra high strength steels (UHSS) has increased. When laser welding UHSS ssheets, heating and cooling of the material will cause geometrical distortions and may cause low joint quality. 700 mm long U-beam structures of 1 mm thick boron steel simulating structural pillars in body-in-white constructions have been laser welded along the flanges with different welding speeds to investigate distortions and weld quality. The results show that final distortions appear in the range of 0-8 mm. FE simulation methods have also been presented which generally predict the distribution of welding distortions.

Keywords: Laser welding, distortion, UHSS, simulation, automotive

1. INTRODUCTION

1.1. Background

Light weight has been in focus for the automotive industry during several years. Driving forces are lower emissions, reduced energy use and increased performance. Numerous variants of high strength steels have been introduced in the car body, making thinner structures possible without renouncing important properties such as strength, stiffness and the ability to absorb high energy at impact situations.

Ultra-high strength (UHSS) press-hardened and hot-formed boron-alloyed steel is commonly used by automotive industry as a mean of reducing weight and increase crash performance. Apart from the unique process technology during forming, it also contains specific alloy elements in order to guarantee a high ultimate strength. During welding of high strength press-hardened body components, weld quality is important and can be difficult to assure. In addition, due to difficult post-welding straightening of the material, welding distortions are important to keep low. In Fig. 1 the trend of increasing use of boron steels can be seen from Volvo Cars Corporation.

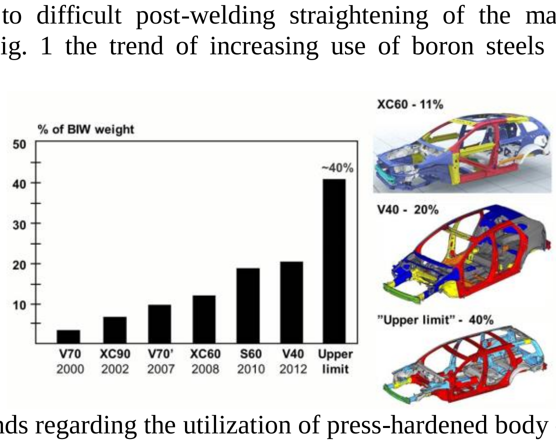

Fig. 1. Development trends regarding the utilization of press-hardened body components at Volvo Car Corporation (Fahlström and Larsson, 2013).

UHSS is suitable in several applications within the automotive industry such as front and rear bumper beams, door reinforcements, windscreen upright reinforcements, B-pillar reinforcements, floor and roof reinforcements, and roof and dash panel cross members (Arcelor Mittal, 2010). The further striving for lighter structures is forcing the automotive producers to use innovative ways to achieve the wanted weight to strength ratio of the design. Unchanged performance properties with thinner and lighter material are a critical issue that has been under great focus the past years. Researchers and material producers all over the world are looking for new ways of designing materials that have higher strength but still are suitable for structures in automotive industry. Objectives like weight reduction, safety and crashworthiness, high formability, cost reduction and sustainable are targeted (Fahlström and Larsson, 2013).

A common method for joining these materials is laser welding. Laser welding can be described as a high productivity welding method suitable, with respect to general welding speed and strength properties, for UHSS as well as most automotive applications. The method is usually a compliment to resistance spot welding (RSW) which historically has been the most used method for joining for body-in-white applications due to its low cost and high ability of automation. Laser welding is associated with low heat input but also high cooling rates which strongly affects the material being welded. In addition, laser welding, as opposed to RSW, creates a narrow and continuous weld which is associated with high strength. (Fahlström and Larsson, 2013).

Due to the introduction of heat into the material and asymmetrical structures, welding will cause expansion and shrinkage to result in unwanted remaining geometry changes in the design. It is necessary to control distortions and minimize residual stresses in the material, or ensure that the design compensates them. If not, geometrically important points for assembly can be displaced several millimeters resulting in gaps and low product quality.

Several methods for prediction of welding distortions have been presented. Early research focused on empirical and simplified local models to predict distortions of idealized geometries (Verhaeghe, 1999). While such models were helpful for practical engineers they were often too simplistic to accurately predict distortions in many applications. During the last decades research on prediction of welding distortions has focused on numerical methods and Finite Element (FE) models in particular (Lindgren, 2001). Many papers model the welding process in a thermo-mechanical transient simulation, where the laser beam is modeled as a conductive heat source. However, in order to reduce computation times and pre-processing efforts, research has also focused on simplified FE models where the heat source is approximated as a temperature gradient, which causes displacements due to pure thermal contraction strains. Early studies (Bachorski, et al., 1999) investigated the technique for gas metal arc welding of 6 mm plain carbon steel sheets and concluded that the magnitude of distortions can be accurately predicted. Another study (Tikhomirov, et al., 2005) compared different simulation techniques to predict MAG-welding distortions of an industrial steel control arm in a T-joint configuration. It was concluded that the simplified technique greatly reduced computations times and with proper calibration could predict distortions with good quantitative agreement. A third study (Camilleri, et al., 2006) evaluated the temperature gradient simulation technique on 6 mm fillet welded of a steel with a yield strength of approximately 220 MPa at ambient temperature. Again, the significantly reduced computation times were stressed and the predictions were concluded to be reasonbly accurate.

The present study treats laser welding of thin UHSS sheets in overlap welding. Thus, several process conditions, which have not been investigated by simplified simulations before are introduced. This work will further examine the capacity and range of simplified simulations of welding distortions.

1.2 Aim of paper

The aim of this paper is to investigate where, and to what extent and form, distortions occur while laser welding press-hardened boron steel. Different welding speeds will be used to see the influence of heat input. Welding will be done on hat profile beams simulating A-pillars and B-pillars in automotive structures. The paper aims to assess the predictive capability of a simplified and time efficient FE model for distortions of thin UHSS beam structures after welding and unclamping.

2. EXPERIMENTAL METHODS

2.1 Material

In the present study MBW 1500P steel with AlSi coating (+AS) was used, delivered from ThyssenKrupp Steel. The steel was hot formed into a beam-geometry which in combination with a flat sheet could be altered into two geometries generating two different distortion modes. One beam should give possibility to asymmetric deformation when joining a hat-profile with a flat sheet (hereafter named “single hat”), and the other symmetric deformation along the neutral plane of the geometry when joining two hat-profiles (hereafter named “double hat”), see Fig. 2. The two cases were chosen as simplified models to simulate A- and B-pillars. Detailed geometry of the hat profile can be seen in the right figure in Fig. 3. Thickness of the material was 1.0 mm and a beam length of 700 mm.

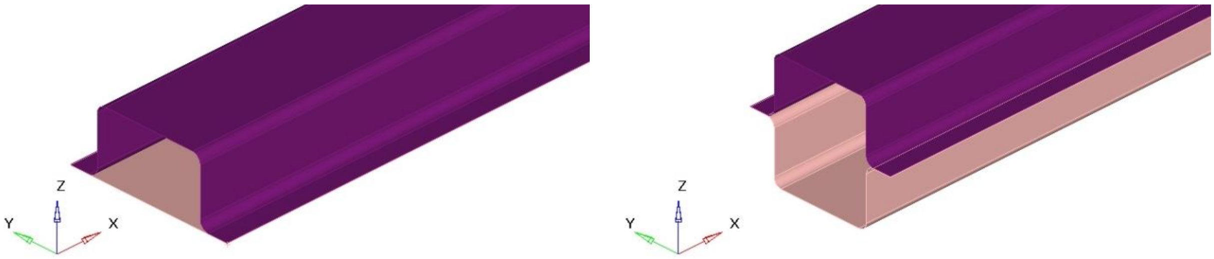

Fig. 2. Geometries chosen as type cases, single hat (left) and double hat (right).

2.2. Fixture and welding sequence

The beam was mounted in a robust fixture. The fixture holds the flanges with 5 clamps evenly distributed on each flange, using pneumatics. Clamping force was set individually for each clamp. The welding was done at the center of the flange in opposite directions for the two sides. The clamping range was 3 mm in from the flange edge. The full sequence consisted of welding, cooling for three minutes, and then unclamping with 10 seconds between unclamping each pair of clamps starting from one end. The last clamping pair (H1 + V1) was unclamped after 30 seconds instead of 10 seconds. The sequence is illustrated in Table 1.

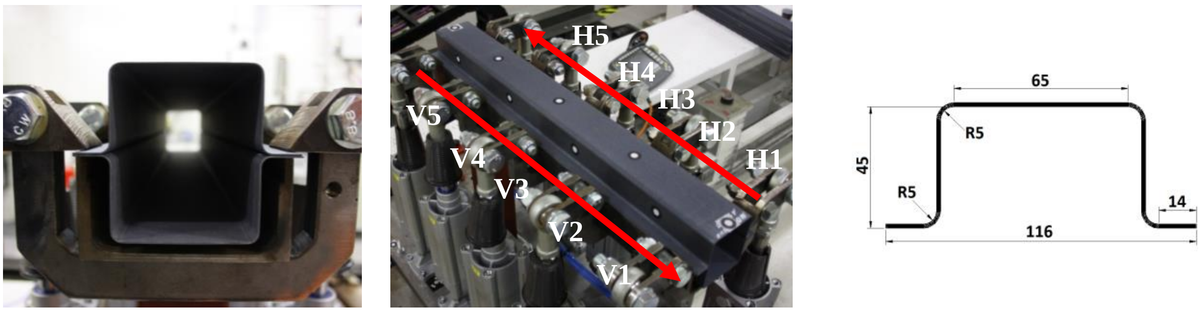

Fig. 3. Left and middle picture shows the fixture used during welding trials. In the middle picture the welding direction on each flange can be seen including each clamping H1-H5 and V1-V5. In the right picture the dimensions of the 700 mm long beam are shown in detail (shown in mm).

Table 1. Describing the welding and unclamping sequence.

Welding during 11/24/55 sec depending on welding speed	Cooling during 180 sec	Unclamping pair H5 + V5	Unclamping pair H4 + V4 after 10 sec	Unclamping pair H3 + V3 after 10 sec	Unclamping pair H2 + V2 after 10 sec	Unclamping pair H1 + V1 after 30 sec

The pneumatic clamping was set on 4 bars to ensure sufficient force holding the beams. A lower clamping pressure resulted in separation of the sheets at the faying surface and the gap caused cutting effects from the laser beam. Parameters from the laser welding process can be seen in Table 2. Three setups were used only varying the welding speed to create different heat inputs to the material.

Table 2. Parameters used during laser welding.

Welding speed (m/min)	**Power (W)**	**Focal position**	**Spot size (µm)**	**Laser source**	**Optics**	**Travel angle**
1.5	4000	Surface	600	HL4006D	Permanova 200/200	0º
3.5	4000	Surface	600	HL4006D	Permanova 200/200	0º
7.5	4000	Surface	600	HL4006D	Permanova 200/200	0º

2.3. Measurement of distortions

After the welding sequence, cooling and unclamping the beam geometry was measured. The total height and width of the beam was measured at three different locations, at each end of the beam and in the middle. See Fig. **4**. When measuring the width of the beam the flanges were included. The measurement was done with a Vernier caliper. All experiments were repeated three times using the mean measurement for analysis.

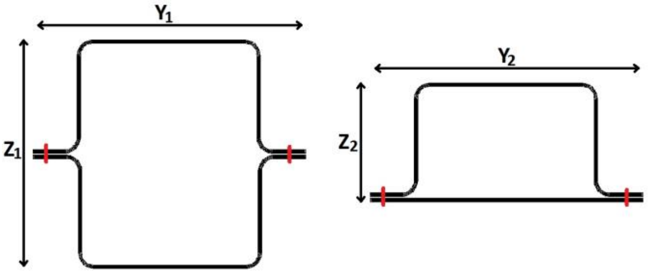

Fig. 4. Measurements of welding distortions. Y_1, Z_1, Y_2 and Z_2 were noted for three positions on the beam; in both ends and in the middle of the beam.

3. EXPERIMENTAL RESULTS

3.1 Joint quality

During welding three different welding speeds were used. Representative cross-sections from these can be seen in Fig. **5**. For welding speed 1.5 m/min (left) the molten material has sunk in the cross-section (commonly known as sagging). Welding speed 3.5 m/min (middle) shows a quite common look of a laser welded thin sheet material. Welding speed 7.5 m/min (right) shows a partially penetrated weld. In conclusion, the results shows that decreased welding speed increases metallurgical impact and may cause weld discontinuities. Consequently, increased welding speed reduces metallurgical impact but will also reduce penetration depth, which may lead to insufficient joint strength.

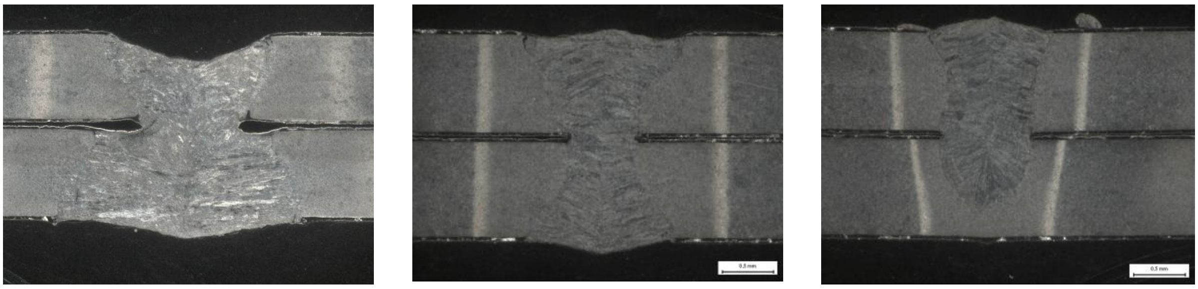

Fig. 5. Cross sections of samples welded with travel speed 1.5 m/min (left), 3.5 m/min (middle) and 7.5 m/min respectively.

The rapid cooling from the laser welding process results in fully martensitic structure of the weld. After welding the material rapidly cools resulting in quenching times faster than for diffusion to occur in larger extent. This results in locking of a microstructure which equals to hard martensite (Zhao et al. 2013).

3.2 Distortions

In general, two different characteristic distortion modes occurred for the two geometries welded, see Fig. 6. The single hat beam suffered from transverse shrinkage of the gap between the “legs” of the profile. This resulted in a small height change at the ends of the beam. The reason for the height change specifically at the ends is that the built in heat from the process increases along the flange. Something that also was noted was an occasionally low weld quality between the clamps. In these areas the profile has risen from the flat sheet giving a gap resulting in cutting with the laser process.

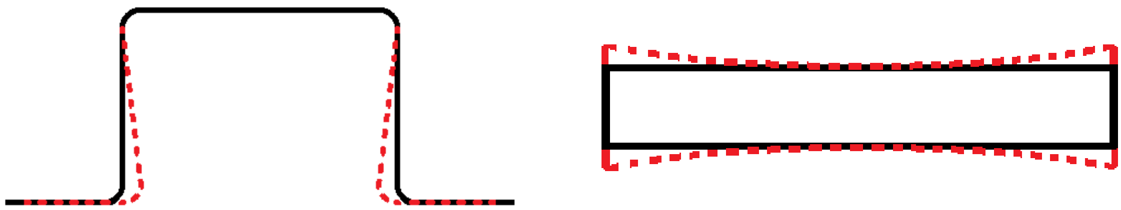

Fig. 6. Dominant geometrical distortions occurring after welding for single hat (left) and double hat (right).

The double hat beam suffered from larger distortions than the single hat beam. In this case the geometrical change was in the transverse direction with a hourglass looking shape. Due to the geometrical symmetry of the beam before welding the distortion did not result in a longitudinal bending mode as for single hat, rather expansion of the cross-section width.

In Fig. **7** the measured values of the distortions can be seen. An average value of three repetitions is shown. The results show overall low scatter. For the single hat beam the distortion were small, with a maximum value of around 1.0 mm. For double hat beam the distortions were several magnitudes larger, with maximum around 8.0 mm. For the double hat beam it was clear that a higher heat input resulted in a larger distortion. The results show the effect of the plane sheet of the single hat geometry which increases the stiffness of the geometry, and reduces distortions.

In conclusion, the results show that welding speed significantly affects magnitudes of distortions in the double hat geometry. In addition, in the single hat geometry the distortions are generally smaller compared to the double hat geometry. Thus, the results suggest that welding distortions may be mitigated by advantageous design of structures or optimized process parameters.

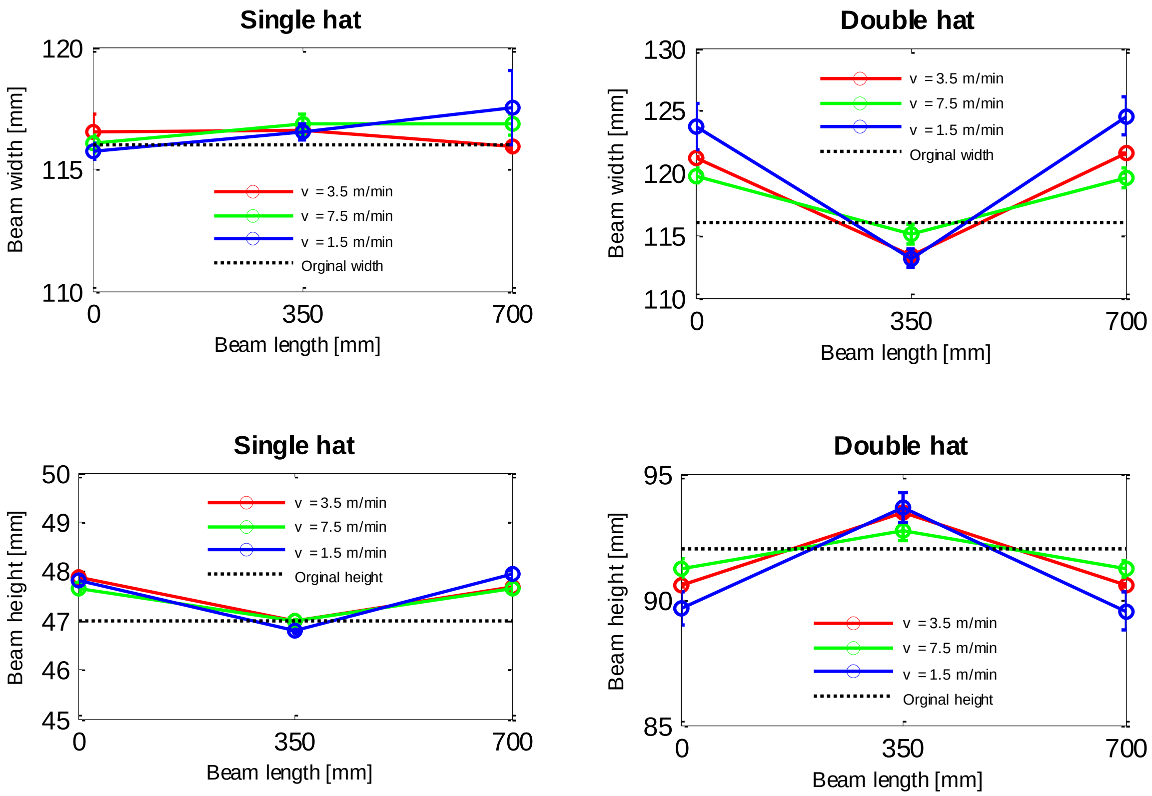

Fig. 7. Remaining deformation from welding in both single and double hat geometry. The distortions (height and width) are measured by a Vernier caliper at the edges and in the middle of the beam.

4. SIMULATION TECHNIQUES

An FE model was generated and simulations were performed using ESI Group's Weld Planner. The model consists of quadrilateral shell elements (type: Q4γ) connected with 6-DOF spring elements at the weld line to connect the upper and bottom sheets in the overlap weld, see Fig. **8**.

In order to simplify the simulation and reduce computation times, laser heat source is modeled as a negative temperature gradient at the region near the weld. Previous researchers have suggested that the temperature gradient should be imposed at the plasticized zone near the weld (Camilleri, 2006). However, as the plasticized zone is difficult to obtain, it is assumed that the plasticized zone is twice as wide as the weld, as recommended by ESI (ESI Group, 2013).

The weld width was obtained from metallographic sections and measurement at the mid-thickness of the sheets from the 3.5 m/min weld results. Fig. **9** illustrates the weld sizes at the mid-thickness of the double and single hat geometries. The temperature gradient was imposed at an area twice the size of the weld width in the transverse direction assuming the plasticized zone.

The clamping is modeled by constraining the displacement in all directions to zero at the nodes near the clamps. After the temperature gradient has been imposed the boundary conditions of the clamps are released as in the experimental procedure. The simulations are performed step-wise, as described in Table 3, to model the welding and unclamping. In the final step a boundary condition, which hinders downward displacement of the bottom flange was imposed. This step models the beam resting on the fixture after unclamping.

Table 3. Loads and boundary conditions of finite element model computation steps.

Computation step	1	2	3	4	5	6	7
Temperature gradient	1st weld	2nd weld	-	-	-	-	-
Locked boundary conditions	All	All	H1-H4 V1-V4	H1-H3 V1-V3	H1-H2 V1-V2	H1 V1	-

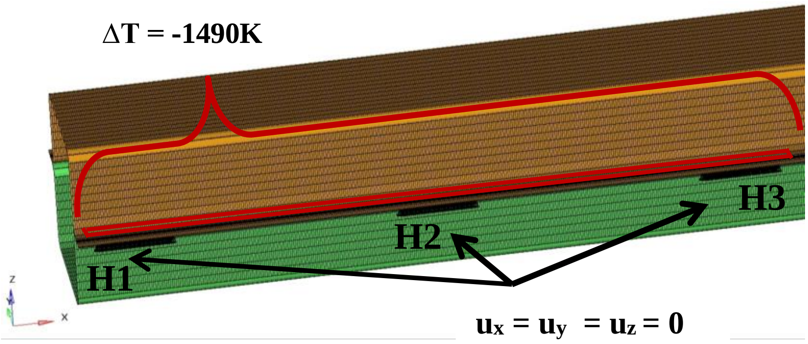

Fig. 8. Part of FE model.

The material model is defined by the elastic parameters (E = 210 GPa, v = 0.3), yield strength (σ_Y = 1143 MPa) and a plastic flow curve ($\sigma_{pl} = 769\varepsilon^{0.26}$) and the thermal expansion coefficient (α = 1.2e-5 K^{-1}). The temperature gradient is set to ΔT = 1490 K, by defining the solidus temperature as 1783 K and assuming an ambient temperature of 293 K.

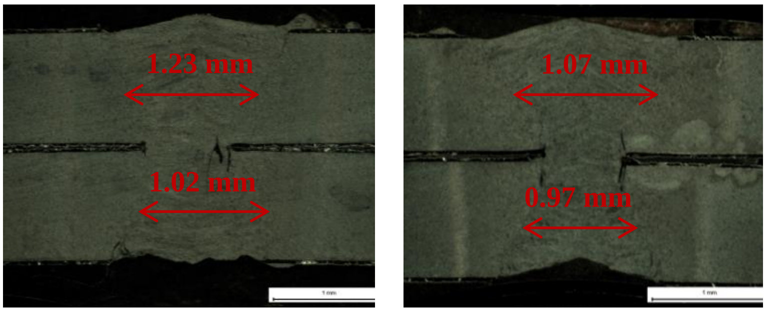

Fig. 9. Cross-sections of 3.5 m/min welds of double hat (left) and single hat geometry (right).

5. SIMULATION RESULTS

After the final simulation step a displacement field is generated, which predicts the geometrical distortions due to welding and unclamping. The simulations were completed in approximately 80 minutes, which is significantly less compared to an equivalent transient simulation. Fig. **10** shows the transverse shrinkage of the cross-section and the transverse shrinkage along the beam along for the two geometries. As seen, the simulations capture the shape of the distortions of the beam. The temperature gradient causes narrowing of the mid-part of the beam and the expansion of the end parts. Consequently, the mid-part is expanded in the vertical direction and the end parts are contracted vertically. The simulations also capture that the double hat geometry experiences greater distortions compared to the single hat geometry due to the stiffness of the flat sheet, which hinders transverse shrinkage.

In conclusion, the simulations show generally good agreement with experiments. They show that a simplified shell model, which relies on ambient temperature material data, can describe the general behavior of laser beam welding distortions. The results indicate that the extension of the temperature gradient can be approximated by twice the weld width to show promising results.

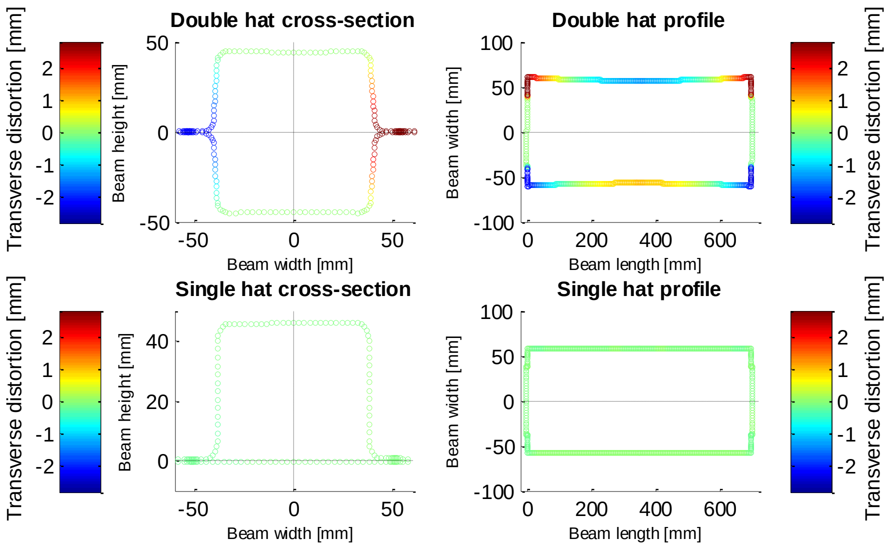

Fig. 10. Results of welding distortions from FE model.

6. DISCUSSION

In the present study distortions due to laser welding of UHSS hat profiles were analyzed. The experiments were performed to simulate laser welding of flanges at A-pillar and B-pillar structures, a common application in automotive design. The two chosen geometries gave two different dominant distortion modes.

In order to analyze the distortions accurately and effectively, the experiments were performed in idealized laboratory conditions. While the results give relevant understanding of the laser welding process, in assembly production other factors affect the process which should be taken into account for industrial implementation.

Firstly, the geometries are simplified compared to actual pillars. Therefore more complex distortions or combination of distortion modes may occur in actual A- and B-pillars. Secondly, the present study uses highly controlled and accurate clamping equipment. However, in actual production more economical clamping equipment is commonly used. A relevant continuation of the present work is to investigate more production-like clamping conditions such as RSW tack welds in combination with pressure wheels and their effect on weld quality and distortions.

As presented above, a higher welding speed resulted in lower distortions and nearly maintained weld width at the interface. However, the penetration depth was also lower and the fusion zone did not reach the root of the weld. Thus, such welds cannot be evaluated visually to confirm joint quality. As no effective non-destructive test method for large scale productions exists, the weld parameters are not suitable for production welding. It is of interest to find alternative methods for confirming weld quality of non-fully penetrated welds to use process parameters to reduce welding distortions.

The distortion modes that occur are resulting in an asymmetrical shape along the length of the beam. For single hat beams the transverse shrinking results in bending of the beam. The magnitude of bending is quite small hence the flat sheet is preventing the distortion to accelerate. As seen in the double hat beam both profiles will deform in transverse direction resulting in an hourglass shape. In this case nothing is limiting the distortion resulting in large shape changes up to 8.0 mm. Tolerances of 8.0 mm distortions are excessive for large scale automotive production. If considering the location of the distortion, this is most likely depending on built in heat along the sequence. The longer the weld is, more distortions will occur. From a production view, this could probably be controlled by stitching if strength and fatigue criteria still are fulfilled.

An FE model was presented which relies on simplifications supported by certain assumptions of the welding process in order to reduce computation times and input data requirements. The geometrical simplification through shell element modeling and the heat source simplification through a discrete temperature gradient will not fully describe the physics of the welding process. For example, through thickness variations of temperature and metallurgical transformations are not captured by the model.

Previous research of simplified models of welding distortions, investigated other welding methods, sheet materials and joint configurations. As the previous investigations, the present study shows that the simplified simulations can quantitatively predict and show the distortional behavior of the structure due to welding. The simulations are also completed in a reasonable time span for industrial implementation for welding engineering work. For a full understanding of the limitations of the simplified approach for a specific case, a full transient analysis should be performed and compared to the simplified results.

Welding distortions are something that needs to be controlled and understood. Within the automotive industry a shape change of 8.0 mm after welding would result in expensive and complicated additional operations. Distortions could therefore be a stopper for the increased use of laser welding of UHSS. Future work needs to include additional parameter variation, more complex geometries that are similar to used components, as well as understanding of how the distortions occur during the welding process.

7. CONCLUSIONS

From this study the following conclusions can be drawn:

- The trials were performed to simulate laser welding of flanges at A-pillar and B-pillar structures. Two chosen geometries gave two different distortion modes. The geometries are simplified and therefore more complex distortions may occur in actual A- and B-pillars.

- Distortion modes occurring was mainly bending and transverse expansion. The single hat beam suffered from longitudinal bending due to its asymmetric geometry. The double hat suffered from transverse expansion resulting in an hourglass shape of the beam. The maximum single hat distortion was around 1.0 mm in comparison with original geometry while the maximum double hat distortion reaches 8.0 mm. For both geometries the largest deformation occurred in the two ends of the beam and the deformation increased with increased heat input.
- A simplified FE model with shell elements and a simplified heat source formulation was developed to model welding distortions. The results show that the simplified model can be used to assess dominant distortions modes of laser welded beam structures after welding and unclamping. The simulations were completed in a reasonable time for industrial implementation.

ACKNOWLEDEMENTS

The present research was financed by the Swedish Governement Agnecy VINNOVA within the Vehicle research programme FFI under the contract LASERLIGHT which is gratefully acknowledged. Gratitude is also given to the project committee consisting of Anders Ohlsson (SSAB Group), Janko Banik (ThyssenKrupp Steel) and Håkan Sundberg (Volvo Trucks Corporation) as well as the technicians at Volvo Cars, Esa Laurila and Glenn Hopkins.

REFERENCES

Arcelor Mittal (2010), Hot stamping with USIBOR1500P®, AP&T Advanced hot stamping seminar, Detroit, September 15

Bachorski A., Painter M., Smailes A. och Wahab M. (1999), ”Finite-element prediction of distortion during gas metal arc welding using the shrinkage volume approach,” *Journal of Materials Processing Technology,* Vol. %1 av %292-93, pp. 405-409

Camilleri D., Mollicone P. och Gray T. (2006), ”Alternative simulation techniques for distortion of thin plate due to fillet-welded stiffeners,” *Modelling and Simulation in Materials Science and Engineering,* vol. 14, nr 8, pp. 1307-1327

ESI Group (2013), Weld Planner Manual.

Fahlström K., Larsson JK. (2013), Laser welding of 1900 MPa boron steel, Conference proceedings: NOLAMP 14

Lindgren L.-E. (2001), ”Finite element modeling and simulation of welding part 1: Increased complexity,” *Journal of Thermal Stresses,* vol. 24, nr 2, pp. 141-192

Tikhomirov D., Rietman B., Kose K. och Makkink M. (2005), ”Computing welding distortion: Comparison of different industrially applicable methods,” *Advanced Materials Research,* Vol. %1 av %26-8, pp. 195-202

Verhaeghe G. (1999), Predictive Formulae for Weld Distortion: A Critical Review, Woodhead, 1999.

Zhao Y. Y., Zhang Y.S., Hu W. (2013), “Effect of welding speed, on microstructure, hardness and tensile properties in laser welding of advanced high strength steel”, *Science and Technology of Welding and Joining*, vol.18 no.7